

Biophysical study regarding the effect of hydrogen sulfide on molecular structure and DNA of mammalian cornea

Amal E Ibrahim^{1*}, Sahar M. Awad², Shima M. Elshibly², Gehan M. Kamal³

¹Visual Science department, Research Institute of Ophthalmology, Giza.

²Physics department, Faculty of Science (girls), Al-Azhar University, Cairo.

*Corresponding author E-mail: amal.ibrahim2011@outlook.com

Abstract

Background: Humans are affected by both exogenous and endogenous sources of hydrogen sulphide gas (H₂S). Its health effects depend on concentration and the duration of gas exposure. These hazards include-among many effects-eye irritation, tearing and inflammation.

Objectives: Our study aimed to characterize the side effects induced in cornea due to H₂S exposure by using by means of comet assay and Fourier Transformer Infrared Radiation (FTIR).

Materials and methods: sixty chinchilla rabbits were randomly grouped into four groups. Group one served as control. Animals were exposed to hydrogen sulphide gas with concentrations of, 90, 250 and 500 ppm. After exposure, animals were decapitated, and the eyes were enucleated from the eye globe. Their corneas were obtained by sectioning through ora serrate. Corneas were then kept frozen at -20° C for analysis by FTIR spectral and comet assay analysis

Results: NH-OH region changes revealed unusual interface/binding mechanism that related to different surrounding environment as well as co-existence of different formations and conformations in the system after exposure to H₂S gas. Moreover the exposure to H₂S gas has no effect on the CH stretching region that arising from lipid. All parameters of comet assay significantly increase (p<0.05) due to exposed doses. This increase is directly proportional to the increase in exposure level.

Conclusion: Hydrogen sulfide is a very toxic gas to cornea which is considered as window of the eye .it has a serious effect on molecular structure and DNA of cornea. By better understanding its toxicity, we will be able to safely make use of its various benefits without the threat of harm looming over our heads.

Keywords:Hydrogen Sulphide; Eye; Cornea; Fourier Transformation; Comet Assay.

1. Introduction

Hydrogen sulfide (H₂S) is a toxic gas that is flammable, colourless gas and has a terrible smell. It can be produced naturally or artificially from volcanoes, sulfur springs, undersea vents, swamps, stagnant bodies of water, and in crude petroleum and natural gas. H₂S is also associated with municipal sewers and sewage treatment plants, swine containment and manure-handling operations, and pulp and paper operations[1].H₂S can be the product of the natural digestive process[2]. It is responsible for the second highest number of occupational gas-related deaths, after carbon monoxide[3]. Ambient air concentrations of hydrogen sulfide from natural sources range between 0.00011 and 0.00033ppm. Concentrations of hydrogen sulphide in urban areas are generally <0.001 ppm. Much higher levels (often exceeding 0.09 ppm) have been detected in communities living near natural sources of hydrogen sulfide or near industries releasing hydrogen sulphide[4]. Its health effects can vary depending on the level and duration of exposure. Repeated exposure can result in health effects occurring at levels that were previously tolerated without any effect[5]. According to Occupational Safety and Health Administration2017 (OSHA,) permissible exposure limit (PEL) is defined as the maximum air concentration you can be exposedwithout respiratory protection.The time Weighted Average is the average exposure over a specified period, usually hours in an eight hour period, 40 hour week, (TWA) is 10 ppm. Short term exposure limit(STEL) is

the acceptable average exposure over a short period of time, usually based on a 15 minute is 15 ppm. Immediately dangerous to life and health (IDLH) is 100 ppm. The immediate death level which leads to immediately deathin 35 minutes is 1000 ppm. A list of current Threshold Limit Value(TLV) and biological exposure indices (PEIs) are published annually by the American Conference of Governmental Industrial Hygienists(ACGIH).According to ACGIH 2017, TWA andSTEL were 1 ppm and5 ppm, respectively.It is found according to OSHA 2017 that prolonged exposure to hydrogen sulfide may cause tearing of the eyes at 2-5 ppm, by raising exposure to 50 ppm slight conjunctivitis (gas eye) appear, and eye irritation at 100 ppm. Prolonged exposure to hydrogen sulfide, even at relatively low levels, may result in painful dermatitis and burning eyes as reported by Agency for Toxic Substances and Disease Registry 2014(ATSDR).

The present work was aimed to explore the molecular structure of rabbit's cornea and its DNA damage after exposure to different concentrations of hydrogen sulphide using infrared spectroscopy and comet assay.

2. Materials and methods

2.1. Chemicals

Hydrogen sulfide saturated solution was obtained from the ministry of environment, Cairo, Egypt. Other chemicals used in the

experiments were obtained from Sigma Company (St. Louis, MO, USA) with the highest purity grade available unless otherwise mentioned.

2.2. Animals

Sixty healthy Chinchilla rabbits of either sex, weighing 2–2.5 kg were randomly selected from the animal house facility at the Research Institute of Ophthalmology RIO, Giza, Egypt. The animals were kept separately under good ventilation and adequate standard diet. They were housed in special designed cages and maintained under constant air flow and illumination during the experimental periods. The animal was handled according to the ARVO (The Association for Research in Vision and Ophthalmology) statements and regulations for the use of animals in research. The rabbits were divided into 4 groups: control and 3 different exposed saturated H₂S solution of concentration 90, 250 and 500 ppm, respectively.

3. Hydrogen sulfide exposure

Animals were exposed to H₂S gas for one hour in a specially designed chamber. The lid of the glass chamber has two ventilation holes to allow excess H₂S vapor and oxygen to flow. The concentration of the H₂S gas inside the chamber was monitored by the gas alert micro 5 gas detector (Brandt Instruments, Inc. LA, USA).

4. Cornea preparation

Animals were decapitated, and the eyes were enucleated from the eye globe. Their corneas were obtained by sectioning through ora serrate. Corneas were then kept frozen at – 20° C for analysis by FTIR spectral and comet assay analysis.

5. FTIR spectroscopy measurements

The corneas were weighted separately, and then crushed to powder by the aid of liquid nitrogen and mortar. The resulted corneal powder was freeze-dried for 24 h then mixed with potassium bromide (KBr) powder (80 mg KBr: 20 mg cornea) to prepare the KBr disks for analyzed with FTIR measurement. FTIR spectra were recorded using Thermo Nicolet IS5 FTIR spectroscopy, USA in range 4000-1000 cm⁻¹ at roomtemperature as briefly previously described by Eman and eman 2011[6].

6. Single cell gel electrophoresis (comet assay)

For the comet assay, 6 μL of cornea homogenate was used and it is performed according to Nandhakumaret al., 2011 [7].

Statistical evaluation
Results were displayed as the mean ±SD. To obtain a comparison between groups, investigation of fluctuation was done by using the commercially available software program (SPSS-11 for windows, SPSS Inc., Chicago, Illinois, USA), where the significance level was set atP<0.05.

7. Results

The spectra of FTIR results for normal and exposed corneas to specific concentration of H₂S that were recorded in the range

4000-1000 cm⁻¹ are shown in fig.1. The detailed FTIR spectral analysis was performed in a three distinct frequency ranges, 3800-3000 cm⁻¹ (NH-OH region), 3000-2800 cm⁻¹ (CH stretching region) and 1800-1000 cm⁻¹ (fingerprint region). Also amide I band (1700-1600 cm⁻¹) which linked to fingerprint region and related to protein secondary structure was carefully analyzed.

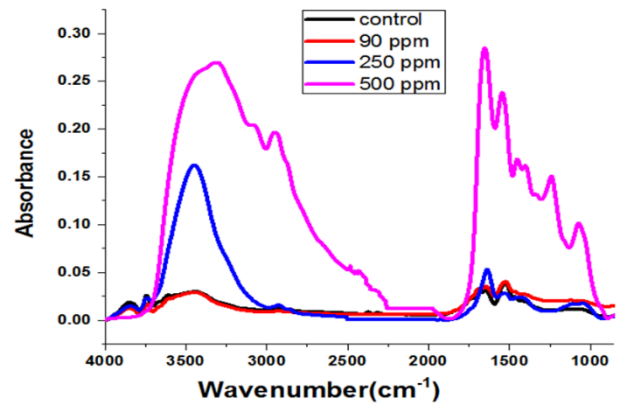


Fig. 1: Full Scale FTIR Spectra for Control and Exposed Corneas of Different Doses of H₂S.

NH-OH region

Fig (2) shows the NH-OH region (3800-3000 cm⁻¹) of corneal tissues. The curve enhancement procedure; a combination of Fourier deconvolution and nonlinear curve fitting resolved the main peak of normal pattern into seven peaks as 3747±3, 3607±2, and 3513±2cm⁻¹ that corresponding to stretching OH (strOH) labeled as (1), the peak at 3432±4 cm⁻¹ related to OH asymmetric (asymOH) that labeled as (2), 3326±3 related to NH asymmetric (asymNH) labeled as (3), 3218±1 cm⁻¹ related to OH symmetric (symOH) labeled as (4), and 3162±1 cm⁻¹ which corresponding to NH symmetric (symNH) labeled as (5) as given in table (1) and previously mentioned by Aly 2011[8].

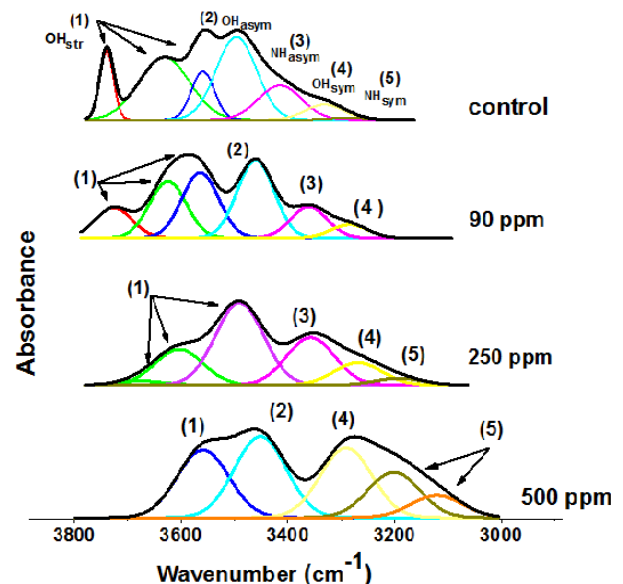


Fig. 2: Analysis of NH-OH Region (3800-3000 Cm⁻¹) for Control and All Corneas Exposed to Different Concentration of H₂S.

Table 1: NHOH Region (3800-3000 Cm⁻¹) of Corneal Tissues for Control and All Groups Exposed to Different Concentration of H₂S

	(1) _{str} OH				(2) _{OH_{asym}}	(3) _{NH_{asym}}	(4) _{OH_{sym}}	(5) _{NH_{sym}}
Control	3747±339±11		3607±2 146±10	3513±2 65±6	3432±4 115±10	3326±3 124±7	3218±1 108±2	3162±1 95±6
90 ppm	3729±2 [†] 93±8 [†]		3610±3 93±11 [†]	3543±3 [†] 93±9 [†]	3425±3 [†] 93±9 [†]	3310±3 [†] 99±8 [†]	3225±1 [†] 96±10	
250		3684±1	3 [†] 59±2 [†]		3478±3	3313±2 [†]	3232±3 [†]	3148±2 [†]

ppm		128±5	109±6 [†]		118±8		118±9 [†]	118±9 [†]		115±7 [†]
500 ppm				3558±4 [†]		3451±2 [†]		3291±1 [†]	3201±2	3120±1 [†]
				114±8 [†]		114±5		114±10	114±9	114±6 [†]

First line in each cell indicates the vibrational frequency, while second line reflects the bandwidth.

[†]statistical significant (p<0.05)

After exposure to different concentrations of H₂S gas, there was remarked change in the counter of NH-OH region. The stretching OH (strOH) in the control rabbit has three bands discernible at 3747±3, 3607±2 and 3513±2 cm⁻¹. Due to exposure to 90 ppm and 250 ppm of H₂S, the same observation can be noticed; there are three peaks but with different characteristic band positions and bandwidth as compared with the control pattern. Finally, at higher dose -500 ppm- there are restriction in the vibrational motion of the NH-OH bands and one peak was detected at 3558±4 cm⁻¹ with significant increase in both band position and bandwidth. For the OH asymmetric (asymOH) mode of vibration, it was found to be sensitive to the exposure to the specific concentrations of H₂S when compared to control pattern. It has significant decrease in band position after exposure to 90 ppm, and significantly increased at 500 ppm. This mode of vibration has been restricted at 250 ppm. Again, The stretching NH asymmetric (asymNH) vibrational mode can be related directly to the exposed doses of H₂S; its band position as well as bandwidth were decreased as the exposure dose increased and finally, it was restricted due to exposure to the highest dose of H₂S (500 ppm). The stretching OH symmetric (symOH) band is sensitive to H₂S exposure. It was located at 3218 ± 1 cm⁻¹ in control pattern, then its band position directly increased with the exposure dose of H₂S. No change in its bandwidth was noticed between groups. Stretching NH symmetric (symNH) vibrational motion was restricted at 90 ppm. As the exposure dose increased to 250 ppm there was a significant reduction in its band position. For the highest dose; 500 ppm, it has been splitted to two peaks with reduced vibrational frequency as given in table (1).

CH stretching region

The CH stretching region of normal corneas and those exposed to H₂S gas is shown in fig. (3). The CH vibrations indicate the presence of four absorption bands at 2963±2 cm⁻¹ with bandwidth 28±5 cm⁻¹, 2925±3 cm⁻¹ with bandwidth 44±6 cm⁻¹, 2879±3 cm⁻¹ with bandwidth 50±9 cm⁻¹, and 2855±3 cm⁻¹ with corresponding band width 40±6 cm⁻¹. These bands assigned as asymCH₃, asymCH₂, symCH₃ and symCH₂ respectively as mentioned by Severcan et al., 2000[9]. The general observation that can be concluded from this figure and table (2) is that exposure to H₂S gas in the concentration range 90 to 500 ppm does not affect the vibrational motion of the CH bond.

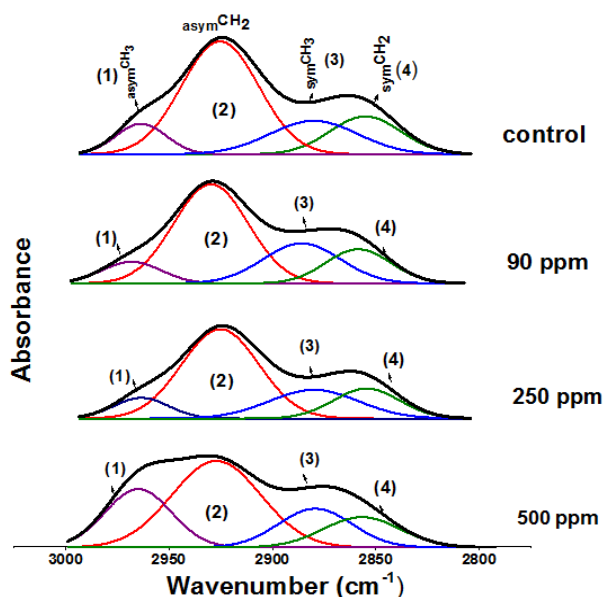


Fig. 3: Analysis of CH Region (3000-2800 Cm⁻¹) For control and All corneas Exposed to Different Concentration of H₂S.

Table 2: CH Region (3000-2800cm⁻¹) for Control and All corneas Exposed to Different Concentration of H₂S

	asymCH ₃	asymCH ₂	asymCH ₃	asymCH ₂
Control	2963±2 28±5	2925±3 44±6	2879±3 50±9	2855±3 40±6
90 ppm	2963±2 33±4	2925±2 42±2	2882±2 44±5	2854±2 37±5
250 ppm	2963±2 31±2	2924±1 44±1	2879±3 51±8	2854±2 38±6
500 ppm	2961±2 34±4	2927±3 46±3	2883±3 38±6	2860±3 40±4

First line in each cell indicates the vibrational frequency, while second line reflects the bandwidth.

Fingerprint Region

The third region of the FTIR in Fig (4) is the fingerprint region (1800-1000 cm⁻¹). Analysis of control pattern revealed the presence of 9 bands at 1727±2, 1646±3, 1520±2, 1457±3, 1388±3, 1335±4, 1289±2, 1151±2 and 1070±1 cm⁻¹ and can be assigned as (1) ester C=O, (2) amide I, (3) amide II, (4) CH₂ bending, (5) stretching_{sym}COO-, (6) deformCH₃, (7) stretching_{asym}PO₂, (8) stretching_{asym}COOC and (9) stretching_{sym}PO₂ as mentioned by Aly 2011[8].

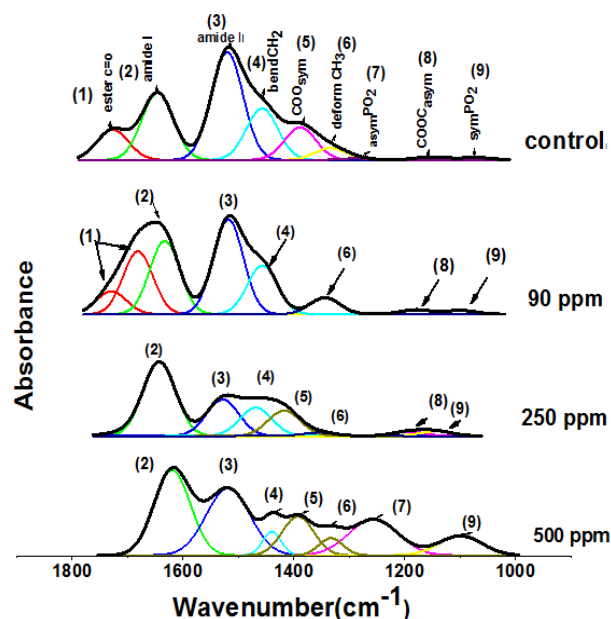


Fig. 4: Analysis of Fingerprint Region (1800-1000cm⁻¹) for Control and All Corneas Exposed to Different Concentration of H₂S.

After exposure to 90 and 250 ppm of H₂S, the vibrational motion of ester C=O that labeled as (1) was increased and splitted in 90 ppm group, and restricted at 500 ppm. Amide I that labeled as (2) and located between 1700-1600 cm⁻¹ attributed to C=O stretching of carboxylic acid of amino acid, show increased band position and bandwidth; a detailed analysis is provided in the next section. Amide II band that labeled as (3) and appears at 1520± 2 cm⁻¹ in normal pattern was increased in wavenumber. This increase is directly proportional with the increased dose of H₂S. No change in bandwidth except for 500 ppm.

The absorption band at 1457 ± 3 cm⁻¹ in normal pattern represents the CH₂ bending and labeled as (4) in fig. (4). It shows no significant changes in its band position and no change in its bandwidth due to exposed to H₂S except for 500 ppm. On the other hand, the absorption at 1388±3 cm⁻¹ which represents the COO symmetric mode of vibration (labeled as 5) show significant increase in its band position as well as its bandwidth for 250 and 500 ppm exposed groups. It was restricted in 90 ppm exposed group

CH₃ deformation mode that labeled as (6) and appeared at 1335 ± 5 cm⁻¹ in control pattern was not significantly changed due to the exposure to different doses of H₂S. The absorption of at 1289 ± 2 cm⁻¹ in normal pattern can be assigned as PO₂ asymmetric that labeled as (6). This band restricted in 90 and 250 ppm exposed groups and detected in 500 ppm exposed group but with reduced band position. The COOC asymmetric band labeled as (8) that detected at 1151±2 cm⁻¹ in the control pattern, shows fluctuated

changes due to exposure to 90 and 250 ppm then, restricted due to exposure to 500 ppm. On other hand the PO₂ symmetric mode of vibration that labeled as (9) and discernible at 1070 ±1 cm⁻¹ in the control pattern was found to react with the H₂S gas non-specifically; there was increased in band position at 90 ppm and 250 ppm groups while reduced at 500 ppm. Its bandwidth was increased at 500 ppm as given in the table (3).

Table 3: Fingerprint Region Assignment to Control and Different Exposed Groups to H₂S

	(1)Ester C=O	(2)Amide I	(3)Amide II	(4)CH ₂ bending	(5)coo _{sym}	(6)CH ₃ deform	(7) _{asym} po ₂	(8)cooc _{asym}	(9) _{sym} po ₂
Control	1727±2 67±6	1646±3 65±3	1520±2 76±6	1457±3 67±3	1388±3 63±	1335±4 62±5	1289±2 66±8	1151±2 64±3	1070±1 63±3
90 ppm	1744±1 [†] 66±5	1694±3 66±4	1526±1 [†] 66±9	1460±2 66±8	1404±3 [†] 78±4 [†]	1342±3 66±8	1169±3 [†] 66±3	1086±2 [†] 66±3	
250ppm	1737±2 [†] 77±5	1656±2 [†] 75±3 [†]	1528±1 [†] 79±5	1461±2 80±5	1404±3 [†] 78±4 [†]	1333±3 70±4	1153±2 79±4 [†]	1099±2 [†] 77±5 [†]	
500ppm		1657±2 [†] 87±4 [†]	1534±2 [†] 105±8 [†]	1453±3 44±5 [†]	1400±2 [†] 76±2 [†]	1334±2 57±5	1247±2 [†] 118±9	1069±1 104±5 [†]	

First line in each cell indicates the vibrational frequency, while second line reflects the bandwidth.
[†]statistical significant (p<0.05).

Amide I band

The amide I absorption is mainly associated with protein amide C=O stretching vibration. Fig.4 display the component band of amide I, which are obtained by curve fitting analysis. Four estimated bands were resolved in normal pattern. The bands were detected 1673 ± 3 cm⁻¹ (β - turn structure, labeled as 1), 1652 ± 2 cm⁻¹ (α - helix, labeled as 2), 1637± 2 cm⁻¹ and 1624± 3 cm⁻¹ (β - sheet, labeled as 3) as previously described by Yang et al., 2005 [10].

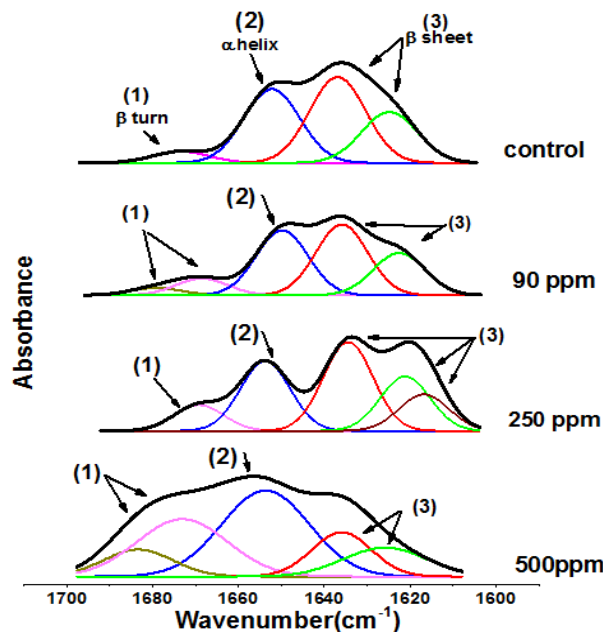


Fig. 5: Analysis of Amide I Region (1700-1600 Cm⁻¹) for Control and All Corneas Exposed to Different Concentration of H₂S.

The contour of the amide I band was affected by the H₂S gas exposure. This change was concomitant with variation in β -turns and β -sheet structures. According to table (5), β -turns content was directly increased as the H₂S exposed dose increased. In the same context, β -sheet was decreased due to exposure to 250 and 500 ppm. The distribution of normal protein secondary structure components (that were calculated as the area percentage) are 5 ± 2 %for β turn, 35± 5 % for α helix and 61± 9 %for β sheet.

Table 4:Protein Secondary Structure Changes of Corneas Expressed as Percentage Area of B-Turn, A-Helix and B-Sheet for Control and All Groups Exposed to Different Concentration of H₂S

Groups	β -Turns%	α - helix%	β - Sheet%
Control	5±2	3±5	61±9
90ppm	12±3 [†]	32±3	56±8
250ppm	1±2 [†]	5±6	5±8
500ppm	36±4 [†]	39±5	25±7 [†]

[†] Statistically significant

Comet assay

The genetic material within the corneal tissue was studied by the Comet assay and the results are given in fig. (6).

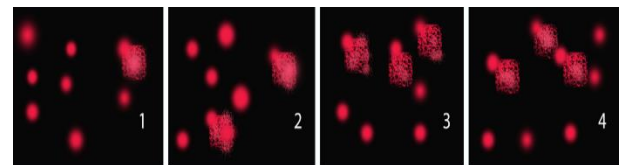


Fig. 6: Representative Photographs of Comet Assay of Cornea Cells for Control and Exposed Cornea for Different Concentration of H₂S 90, 250 and 500 Ppm.

In control group the DNA was tightly compressed and maintained the circular disposition of the normal nucleus. After exposure to the specific doses of H₂S, the profile of the nuclear DNA was altered with the appearance of a fluorescent streak extending from the nucleus as appeared for all doses comprising the comet in different percentages. A variety of symmetrical and densitometric parameters are provided by the image analysis software, which allows an estimation of the amount of DNA in the head and tail region. Because the tail length and its density reflect the number of single-strand breaks in the DNA, the percentage of DNA in the tail provides a quantitative measure of the damaged DNA. The percentage of tailed nuclei, tail length, tail DNA and tail moment in control group and treated groups are given in table (5).

Table 5:Percentage of Tailed Nuclei, Tail Length, Tail DNA and Tail Moment of Exposing Corneas to Different Concentration of H₂S Compared to Control

Groups	%Tailed cells	Tail length(µm)	%Tail DNA	Tail moment(Units)
Control	3±1	0.92±.03	1.29±0.06	1.19±0.06
90ppm	6±1 [†]	1.69± 0.07 [†]	1.82±0.05 [†]	3.08±0.1 [†]
250 ppm	12±2 [†]	2.28±0.1 [†]	2.68±0.2 [†]	6.11±0.5 [†]
500 ppm	17±2 [†]	3.05±0.1 [†]	3.62±0.1 [†]	11.04±1 [†]

†Statistically significant.

The tail length measured from the middle of the nucleus to the end of the tail has smallest value in control group $0.92 \pm 0.03 \mu\text{m}$ (which indicate natural DNA damage). The length increases (statistically increase $p < 0.05$) with doses to reach maximum value $3.05 \pm 0.1 \mu\text{m}$ in 500 ppm. All parameters of comet assay significantly increase due to exposed doses. This increase is directly proportional to the increase in exposure level as given in table (5).

8. Discussion

It is possible to divide the mid-infrared region in other smaller spectral regions where strong absorption bands can be associated to specific components. Those regions are: fatty acids region, amide region, assigned primarily to proteins and peptides; mixed region, assigned to carboxylic groups of proteins, free amino acids; and the polysaccharide region. Besides, there are other spectral regions such as the one that is relevant to RNA, DNA and phospholipid content [11].

The results of this study revealed that the NH-OH region of FTIR spectra (Fig.4) of the corneal tissue is sensitive to exposure of different doses of H₂S.

NH-OH region changes revealed unusual interface/binding mechanism that related to different surrounding environment as well as co-existence of different formations and conformations in the system after exposure to H₂S gas. Changes in OH modes indicate the formation of hydrogen bonds with different structural states [12]. Moreover the exposure to H₂S gas has no effect on the CH stretching region that arising from lipid [13].

The noticeable fluctuation changes in the fingerprint region recognized to an oxidative stress after exposure to different doses of H₂S and increase the stress with the dose. The changing in $\nu_{\text{asym-PO}_2}$ and $\nu_{\text{sym-PO}_2}$ band is indicated to disorder in the genetic material or phospholipids that involved in the structure of corneal tissues which are highly specialized layers.

FTIR spectroscopy has been used to study the secondary structure composition, structural dynamics, conformational changes structural stability and aggregation of proteins. In the amide I region ($1700\text{--}1600 \text{ cm}^{-1}$), each type of secondary structure gives rise to a somewhat different C=O stretching frequency due to unique molecular geometry and hydrogen bonding pattern [14].

For proteins to perform these important tasks, they must fold to their proper, unique three-dimensional structure. Poor protein folding and insolubility lead to inefficient functional protein. There are three common secondary structures in proteins, namely α -helix, β -turns and β -sheets. β -turns are conformations that enable protein to adopt globular structures, and their formation is often rate limiting for folding. They are the smallest type of the secondary structure, joining other elements of secondary structures as α -helix and β -sheets, and abruptly change the direction of the polypeptide chain. The formed β -turn structure may serve as a nucleation site for folding/refolding of proteins. β -sheets are another protein secondary structure conformation; although the importance of β -sheets in the folded structures of

Proteins has long been recognized, there is growing interest of molecular interactions among β -sheets. β -sheets have dual functions; in normal tissue, they are important for biological activities, and they are involved in many diseases such as cancer. Intermolecular β -sheet interactions (band $< 1620 \text{ cm}^{-1}$) are associated with bimolecular recognition, protein quaternary structure, protein-protein interactions and peptide and protein aggregation. While, intramolecular β -sheet interactions (band between $1630\text{--}1620 \text{ cm}^{-1}$) are associated with protein folding [13]. Thus, vibrational spectra, as those of the FTIR spectra, were directly related to the structural features of molecules.

In our study β -sheet the strands of polypeptide are stretched out and lie either parallel or antiparallel to one another and hydrogen bonds forms randomly between the strands after exposure to H₂S. The domination of β -turns content which directly proportion to decrease the content of β -sheet indicates that corneas protein

turns to insoluble and more folded corneal protein which gives the impetus that the proteins become aggregated.

The comet assay for corneal cells has been applied to investigate the potential genotoxicity of H₂S [15].

The degree of DNA damage observed in control group indicated the % tailed cells might be explained by the fact that about 10 000 oxidation hits to DNA per cell have been estimated to occur per day within the human body, and more than 35 different forms of oxidized bases are found in DNA [16].

The effect of H₂S induces p53 (is a well-defined tumor suppressor gene) that has been mapped and characterized in the normal cornea across different species p53 plays a role in many abnormal types of cell proliferation, in apoptosis in response to DNA injury and in the prevention of replication of genomes that have suffered DNA damage [17]. H₂S causes cell cycle alteration and formation of micronuclei (MN). The formation of MN represents fragments of the chromosome or whole chromosomes resulting from clastogenic events and as such is considered as a reliable marker for DNA damage [18]. Also, H₂S triggers important markers of apoptosis, including the release of cytochrome c from the mitochondrial membrane into the cytoplasm and also the translocation of apoptosis regulator Bax gene from cytosol to the mitochondria [19]. Bax play an important role in the regulation of corneal epithelial renewal in adult and during development of cornea [20].

9. Conclusion

Hydrogen sulfide is a very toxic gas to cornea which is considered as window of the eye. It has a serious effect on infra structure and DNA of cornea. By better understanding its toxicity, we will be able to safely make use of its various benefits without the threat of harm looming over our heads.

References

- [1] Xia. Daniel, He. Zhiyong Hydrogen Sulfide (H₂S) in the Permian Basin. Annual Convention and Exhibition, Houston, Texas, United States, April 2-5, 2017 **Data pages © 2017 Serial rights given by author. http://www.searchanddiscovery.com/pdfz/documents/2017/10950xia/ndx_xia.pdf.htm.
- [2] K. Pope, T. So, J. Crane, and N. Bates, Ambient geothermal hydrogen sulfide exposure and peripheral neuropathy, *Neurotoxicology* (2017), 60: 10-15. <https://www.ncbi.nlm.nih.gov/pmc/articles/PMC5447475/>. <https://doi.org/10.1016/j.neuro.2017.02.006>.
- [3] L. Guidotti Hydrogen sulfide: advances in understanding human toxicity, *International journal of toxicology* (2010), 29, 569-581. <http://journals.sagepub.com/doi/pdf/10.1177/1091581810384882>. <https://doi.org/10.1177/1091581810384882>.
- [4] K. Jones, Case studies of hydrogen sulphide occupational exposure incidents in the UK, *Toxicology letters* (2014), 231, 374-377. <https://www.sciencedirect.com/science/article/pii/S0378427414012922>. <https://doi.org/10.1016/j.toxlet.2014.08.005>.
- [5] R. Tiwari, Occupational health hazards in sewage and sanitary workers, *Indian journal of occupational and environmental medicine* (2008)12, 112-115. <http://www.ijoem.com/article.asp?issn=00195278;year=2008;volume=12;issue=3;page=112;epage=115;aualst=Tiwari>. <https://doi.org/10.4103/0019-5278.44691>.
- [6] M.A. Eman and S.A. Eman, Evaluation of prolonged adherent with benzalkonium chloride on corneal protein secondary structure that assessed by Fourier transform infrared spectroscopy *Journal of American Science* (2011)7(12)758-764. https://www.researchgate.net/publication/266886489_Evaluation_of_prolonged_adherent_with_benzalkonium_chloride_on_corneal_protein_secondary_structure_that_assessed_by_Fourier_transform_infrared_spectroscopy.
- [7] S. Nandhakumar, S. Parasuraman, M. Shanmugam, R. Rao, P. Chand, and V. Bhat, Evaluation of DNA damage using single-cell gel electrophoresis (Comet Assay). *Journal of pharmacology & pharmaco-therapeutics* (2011)2, 107. <https://www.ncbi.nlm.nih.gov/pmc/articles/PMC3127337/>.

- [8] M. Aly Effect of different concentration of Benzalkonium Chloride on the cornea, *journal of american science* (2011) 7, 697-703. http://www.jofamericanscience.org/journals/amsci/am0704/97_5298am0704_697_703.pdf.
- [9] F. Severcan, N. Toyran, N. Kaptan, and B. Turan, Fourier transform infrared study of effect of diabetes on rat liver and heart tissues in the CH region, *Talanta* (2000) 53, 55-59. <http://europepmc.org/abstract/MED/18968088>. [https://doi.org/10.1016/S0039-9140\(00\)00379-9](https://doi.org/10.1016/S0039-9140(00)00379-9).
- [10] Y. Yang, J. Sulé-Suso, D. Sockalingum, G. Kegelaer, M. Manfait, and J. El Haj, Study of tumor cell invasion by Fourier transform infrared microspectroscopy, *Biopolymers* (2005) 78, 311-317. <https://www.ncbi.nlm.nih.gov/pubmed/15898120>. <https://doi.org/10.1002/bip.20297>.
- [11] Y. Lin, J. Li, T. Cheng, FT-IR and Raman vibrational microspectroscopies used for spectral biondiagnosis of human tissues, *Journal of Spectroscopy* (2007) 21, 1-30. <https://www.hindawi.com/journals/jspec/2007/278765/abs/>. <https://doi.org/10.1155/2007/278765>.
- [12] A. Morsy, M. Aly, M. Ibrahim, S. Mahmoud, and M. Kamal, Potential hazards of glyphosate on rabbit retina, *Journal of the Arab Society for Medical Research* (2017) 12, 92. <http://new.asmr.eg.net/article.asp?issn=16874293;year=2017;volume=12;issue=2;spage=92;epage=98;aulast=Morsy;type=3>. https://doi.org/10.4103/jasmr.jasmr_10_17.
- [13] M. Gamal, M. Aly, S. Mahmoud, S. Talaat, M. Sallam, FTIR assessment of the effect of Ginkgo biloba leave extract (EGb 761) on mammalian retina, *Cell biochemistry and biophysics* (2011) 61, 169-177. <https://www.ncbi.nlm.nih.gov/pubmed/?term=ftir13> %09Gamal+M.%2C+Aly+M.%2C+Mahmoud+S.%2C+Talaat+S.+and+Sallam+M.%2C+(2011)%2CFTIR+assessment+of+the+effect+of+Ginkgo+bi-loba+leave+extract+(EGb+761)+on+mammalian+retina%2C+Cell+biochemistry+and+biophysics%2C+61%2C169-177.
- [14] J. Kong, S. Yu, Fourier transform infrared spectroscopic analysis of protein secondary structures, *Acta biochimica et biophysica Sinica* (2007) 39, 549-559. <https://www.ncbi.nlm.nih.gov/pubmed/17687489>. <https://doi.org/10.1111/j.1745-7270.2007.00320.x>.
- [15] M. El-Sayed, M. Aly, Toxoplasma gondii infection can induce retinal DNA damage: an experimental study, *International journal of ophthalmology* (2014) 7, 431-436. <https://www.ncbi.nlm.nih.gov/pmc/articles/PMC4067654/>.
- [16] B. Halliwell, Why and how should we measure oxidative DNA damage in nutritional studies? How far have we come?, *The American journal of clinical nutrition* (2000) 72, 1082-1087. <https://academic.oup.com/ajcn/article/72/5/1082/4729758>. <https://doi.org/10.1093/ajcn/72.5.1082>.
- [17] Y. Tendler, R. Pokroy, A. Panshin, and G. Weisinger, protein subcellular localization and apoptosis in rodent corneal epithelium cell culture following ultraviolet irradiation, *International journal of molecular medicine* (2013) 31, 540-546. <https://www.spandidos-publications.com/ijmm/31/3/540>. <https://doi.org/10.3892/ijmm.2013.1247>.
- [18] M. Fenech, and A. Morley, Kinetochore detection in micronuclei: An alternative method for measuring chromosome loss, *Mutagenesis* (1989) 2, 98-104. <https://www.ncbi.nlm.nih.gov/pubmed/2659933>. <https://doi.org/10.1093/mutage/4.2.98>.
- [19] R. Baskar, L. Li and K. Moore, Hydrogen sulfide induces DNA damage and changes in apoptotic gene expression in human lung fibroblast cells, *The FASEB Journal* (2007) 21, 247-255. <https://www.ncbi.nlm.nih.gov/pubmed/17116745>. <https://doi.org/10.1096/fj.06-6255com>.
- [20] S. Roberts, S. Thomas and C. Dorman, Gene expression changes following acute hydrogen sulfide (H₂S)-induced nasal respiratory epithelial injury, *Toxicological pathology* (2008), 36, 560-567. <http://journals.sagepub.com/doi/10.1177/0192623308317422>. <https://doi.org/10.1177/0192623308317422>.